

Full paper / Mémoire

Surface treatment and corrosion behaviour of Fe–32Mn–6Si shape memory alloy

Amin Charfi ^a, Tarak Bouraoui ^{a,*}, Mongi Feki ^b, Chedly Bradai ^a, Bernard Normand ^c

^a *Laboratoire des systèmes électromécaniques, ENIS, B.P.W 3038, Sfax, Tunisia*

^b *Unité de chimie industrielle et matériaux, ENIS, B.P.W 3038, Sfax, Tunisia*

^c *Laboratoire MATEIS, INSA, 21, av. Jean-Capelle, 69621 Villeurbanne cedex, France*

Received 25 August 2007; accepted after revision 26 November 2007

Available online 14 January 2008

Abstract

Fe–Mn–Si-based shape memory alloys are characterized by a good shape-memory effect, but with a modest corrosion resistance. The goal of this study is to try out a suitable surface treatment in order to improve the corrosion resistance of the Fe–32Mn–6Si alloy without impairing its shape-memory properties. The implemented solution is a zinc-electrodeposited coating achieved by chromium conversion treatment. The results show, thanks to electrochemical and thermomechanical measurements, and corrosion tests performed in salt spray chamber, that zinc-electrodeposited coating followed by chromium conversion layer can be considered as a good anticorrosion solution of the Fe–32Mn–6Si alloy. **To cite this article:** A. Charfi et al., *C. R. Chimie 12 (2009)*.

© 2007 Académie des sciences. Published by Elsevier Masson SAS. All rights reserved.

Résumé

Les alliages à mémoire de forme de type Fe–Mn–Si sont caractérisés par un bon effet mémoire de forme, mais par une faible résistance à la corrosion. Le but de cette étude est d'envisager un traitement de surface approprié permettant d'améliorer la résistance à la corrosion de l'alliage Fe–32Mn–6Si sans altérer sa propriété de mémoire de forme. La solution mise au point est un revêtement électrolytique de zinc, suivi d'un traitement de chromatisation. Les résultats montrent, grâce aux mesures électrochimiques et thermomécaniques et aux essais de corrosion réalisés dans une chambre de brouillard salin, que le revêtement de zinc électrolytique suivi d'un traitement de chromatisation peut être considéré comme une bonne solution anticorrosion de l'alliage Fe–32Mn–6Si. **Pour citer cet article :** A. Charfi et al., *C. R. Chimie 12 (2009)*.

© 2007 Académie des sciences. Published by Elsevier Masson SAS. All rights reserved.

Keywords: Shape memory alloys; Zinc coating; Corrosion

Mots-clés : Alliages à mémoire de forme ; Revêtement de zinc ; Corrosion

* Corresponding author. Current address: Institut préparatoire aux études d'ingénieurs de Monastir, route Ibn El Jazzar, 5019 Monastir, Tunisia.

E-mail addresses: tarak.bouraoui@ipeim.rnu.tn, tarak.bouraoui@gmail.com (T. Bouraoui).

1. Introduction

Shape-memory alloys (SMAs) are known primarily for one fundamental and unique property: the

shape-memory effect (SME). This remarkable property consists in the capacity of the SMA to recover a memorized shape by simple heating.

In addition to the classical non-ferrous (Ni–Ti) and copper-based alloys, recently iron-based SMA have attracted much attention because of their low cost, high mechanical strength and good formability [1–3].

The first compositions of iron-based SMA which exhibit a good SME are Fe–Mn–Si system-based alloys containing 28–32% of manganese and 5–6.5% of silicon [2].

The development of these alloys is impeded by their limited corrosion resistance [4]. Recently, other compositions of iron-based SMA have been developed with additions of chromium and nickel. These new nuances present a clear improvement of corrosion resistance. However, the cost of the alloy becomes sometimes less attractive for less interesting performances [5,6].

Therefore, the goal of this study is to try out a suitable surface treatment in order to improve the corrosion resistance of the Fe–32Mn–6Si without impairing the shape-memory property.

It is important to specify here that the present research is undertaken from the viewpoint of “single-use actuator” application type. The coating is set up before prestrain and must protect the alloy against corrosion after prestrain and until the moment of the application works. When the application is operated, the coating should not impair the SME and should not obstruct the spreading of the alloy. The application will thereafter be replaced.

After a preliminary study of the electrochemical behaviour of the Fe–32Mn–6Si alloy and the influence of microstructure on its corrosion sensitivity, zinc electroplating coating was tried out and tested from an anticorrosion point of view. Furthermore, because the interest of SMAs lies in their integration in industrial applications, the anticorrosive performance of the coated SMAs was evaluated in salt spray chamber after prestrain, where the atmospheric corrosion phenomena are highly accelerated. Moreover, in order to verify if the surface treatments do not impair the thermomechanical properties of the alloy, SME was measured before and after coating by a cylindrical mandrel.

2. Material and experimental procedure

The SMA used in this study was obtained from the Aubert & Duval Company. The alloy was supplied as $18 \times 18 \text{ mm}^2$ swaged bars and water quenched at

1373 K. The chemical composition of this polycrystalline alloy is given in Table 1.

This nuance is considered as the reference of iron-based SMAs. The silicon content of 6.45% is justified by the fact that this value is optimal to have a weak stacking fault energy favourable to the reversibility of the $\gamma(\text{fcc}) \rightarrow \varepsilon(\text{hcp})$ martensitic transformation [7].

The transformation temperatures determined by electrical resistance measurements are specified in Table 2 [1]. We notice that the martensite start (Ms) is slightly lower than room temperature. This condition is necessary to obtain a stress-induced martensite at room temperature and is favourable to a good SME [8]. In addition, it should also be specified that martensite finish (Mf) does not correspond to the end of martensitic transformation, but to the stop of its progression. Below Mf, the studied alloy is still a mixture of austenite and martensite. This phenomenon is in relation with magnetic considerations [1].

The samples were cut by an electroerosion machining along the bar direction, mechanically polished and maintained at 873 K for 1 h and then water-cooled at room temperature. After this reference heat treatment, the alloy presented an austenitic structure.

The surface coatings performed for SMAs were zinc electroplating accomplished in a commercial acid chloride bath achieved (or not) by chromate conversion.

The Zn electroplating processes were performed in a laboratory as follows: mechanical polishing, washing in ethanol, water washing, zinc electroplating at 20 mA cm^{-2} for 19 min, water washing and hot-air drying (at about 320 K for 30 s). The Zn electroplating solution was acidic and consisted of 70 g/l of ZnCl_2 , 235 g/l of KCl and 25 g/l of H_3BO_3 . The pH of solution was equal to 5.2 and the temperature used was 300–308 K. The zinc coating thickness was fixed and controlled at 10 μm .

Chromate conversion treatments were performed after Zn electroplating. The samples were activated in 0.5% HNO_3 for 20 s then water washed before the trivalent chromate conversion treatment by immersion in a commercial solution (Tripass ELV 1000, 130 ml/l, pH = 1.6) for 120 s at 333 K. This solution is free from hexavalent chromium and fluoride compounds. The coatings were then water washed and hot air dried (at about 320 K for 30 s).

Table 1
Chemical composition of studied alloy (mass content in %)

Fe	Mn	Si	C
Bal.	31.6	6.45	0.018

Table 2
Transformation temperatures of the studied alloy

Ms ± 5 K	Mf ± 5 K	As ± 5 K	Af ± 5 K
270	215	385	395

Ms: martensite start; Mf: martensite finish; As: austenite start; Af: austenite finish.

Microscopic analyses of Zn electroplated coatings finished (or not) by chromate conversion treatments were performed by Scanning Electron Microscopy using a Philips XL Model 30 at an accelerating voltage of 30 kV.

The electrochemical behaviour of the coated and non-coated SMAs was tested in a 0.5 M Na₂SO₄ solution at pH 4. A representative sample area of 0.28 cm² was chosen for testing. A three-electrode setup was used to study the corrosion behaviour of the samples. Pt was used as the counter electrode. Potentials in this study were referred with respect to the saturated calomel electrode filled with a KCl solution. The electrochemical behaviour of the samples was monitored by measuring the polarization resistance (R_p) using Voltmaster 4 software with a PGP 201 potentiostat/galvanostat. The potential was varied 10 mV above and below the open-circuit potential of samples at a scan rate of 0.5 mV/s [9].

The uniform corrosion of the non-coated alloy was evaluated, in different states, by comparison with AISI 316L stainless steels, by the immersion in a 0.5 M Na₂SO₄ solution at pH 4. The weight loss of the sample was determined by calculating the weight difference of the sample before and after the immersion tests for 200 h.

Salt spray tests were carried out using a neutral 5%_{m/v} NaCl solution sprayed with an atomizer with a nozzle pressure of 0.8–1.6 bar. The samples were arranged in a salt spray cabinet and exposed according to ASTM B 117-97 [10]. The temperature inside the chamber was maintained at 308 ± 2 K.

The shape-memory effect was highlighted and measured by a bending test using a cylindrical mandrel tester. The schematic diagram of the bending experiment is shown in Fig. 1. The sample was fixed at one extremity (position 0) and bended around a steel rod to 90° (position 1). After unloading (position 2), the sample was heated at 623 K for the reversion of stress-induced γ/ϵ martensite (position 3).

The imposed strain depends on the diameter of the bending rod (D) and the thickness of the sample (t). The maximum strain in the top fiber can be estimated approximately by $\epsilon = t/D$.

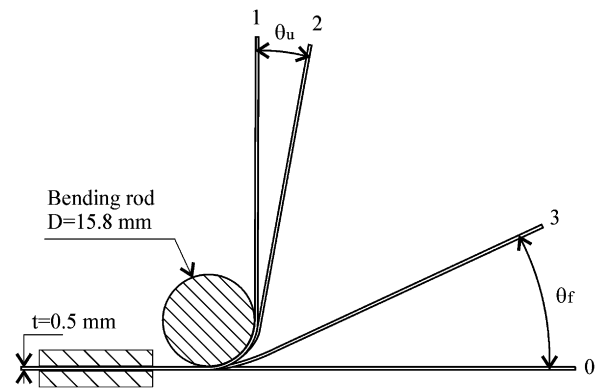


Fig. 1. Schematic illustration for SME measuring by bending (θ_u : unloading angle, θ_f : final angle).

The shape memory ratio, r , is determined by:

$$r[\%] = \left[1 - \frac{\theta_f}{90 - \theta_u} \right] \times 100 \quad (1)$$

where θ_f and θ_u are, respectively, the final angle (after heating) and the unloading angle.

The interest to adapt the mandrel tester, generally used to estimate the adherence of coating, lies in the fact that this original experimental protocol makes it possible, at the same time, to measure the SME and to estimate the adherence of the coating.

3. Results and discussion

3.1. Corrosion testing and electrochemical behaviour of the as-received Fe–32Mn–6Si

A comparison between the polarization resistance of the as-received studied alloy and that of a stainless steel is presented in Fig. 2. It is evident from the curves of Fig. 2 that the studied alloy is much more active than stainless steel in the used solution. The polarization resistance of the as-received Fe–32Mn–6Si is very weak (450 Ω cm²) compared with that observed for stainless steel (28000 Ω cm²). These results agree with previous corrosion studies of iron-based SME [11] and justify the importance of finding an anticorrosive solution before considering the use of this material in industrial applications.

Moreover, insofar as the SME is in relation with $\gamma \leftrightarrow \epsilon$ reverse martensite transformation, it is important to know more about the influence of the microstructure and the involved phases on corrosion resistance. With this intention, the polarization resistance was measured and the uniform corrosion of the non-coated sample was investigated, by immersion in 0.5 M Na₂SO₄ solution at

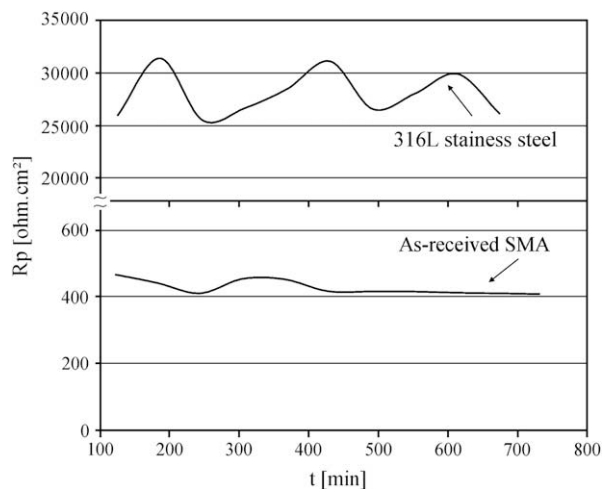


Fig. 2. Polarization resistance of as-received studied alloy and stainless steel.

pH 4 for 200 h at room temperature, in three different states: after reference heat treatment (austenite γ), after reference heat treatment followed by immersion in liquid nitrogen (mixture of austenite γ and thermal martensite $\varepsilon_{\text{thermal}}$) and after reference heat treatment followed by 5% prestrain in tensile (mixture of austenite γ and stress-induced martensite $\varepsilon_{\text{stress-induced}}$). The experimental results are stated in Table 3.

The presence of thermal martensite seems not to affect the polarization resistance. The R_p values of austenite state and austenite + thermal martensite two-phase state are comparable and equal to 440 and 450 $\Omega \text{ cm}^2$, respectively. On the other hand, we noticed a more significant R_p value for the austenite + stress-induced two-phase state. This tendency is validated by the weight loss test. The weight loss of the austenite state and austenite + thermal martensite two-phase state are similar and equal to 17 g/m^2 , while the value for austenite + stress-induced two-phase state is relatively less significant and equal to 11.87 g/m^2 .

The polarization resistance of a given alloy is in relation with its electrical resistivity. For the Fe–32Mn–6Si shape-memory alloy, we have already shown that

the electrical resistivity of the martensitic state is definitely higher than that of the austenitic state [1]. This would explain the apparent corrosion resistance of the martensitic phase. In addition, the fact that the presence of thermal martensite does not affect the polarization resistance would be related to the quantity of the involved thermal martensite. Indeed, a little quantity of martensite was obtained by cooling, because the $\gamma \rightarrow \varepsilon$ martensitic transformation cannot occur, even if the temperature is further reduced. The reason is that the Gibbs energy of austenite is decreased by the antiferromagnetic transition and consequently the driving force available for the martensitic transformation decreases and the transformation is impeded or suppressed [2,12].

In conclusion, our results corroborate that the electrochemical properties of martensite are favourable to a better uniform corrosion resistance. This result does not exclude the possibility of having, for the austenite + martensite two-phase state, a sensibility to pitting corrosion. It has been reported that the duplex alloy of austenite and martensite can be intrinsically less resistant to pitting corrosion than austenite alone [13].

3.2. Surface coating

The average values of polarization resistance determined from results relative to coated and non-coated Fe–32Mn–6Si samples are reported in Table 4.

According to these results, we noticed that the zinc coating reduces the polarization resistance of the studied alloy. It is well known that zinc is more electro-negative than iron, and therefore the protection of the iron-based alloy by zinc is galvanic. Hence, the corrosion protection of Fe–32Mn–6Si by zinc coating can be considered in a sacrificial manner. However, when zinc coating is followed by chromate conversion treatment, the polarization resistance increases. The chromium layer passivates the zinc coating with the formation of a thin, although adherent and efficient layer, improving the corrosion resistance of the zinc layer.

A scanning electronic microscope was used to visualize the coatings microstructure. Fig. 3 represents the microstructure achieved on samples of SMAs coated with zinc and coated with zinc and converted by chromium.

Table 3

Corrosion behaviour of SMA in different states compared with stainless steel

Fe–32Mn–6Si states	R_p ($\Omega \text{ cm}^2$)	Weight loss (g/m^2)
γ	440 ± 10	17
$\gamma + \varepsilon_{\text{th}}$	450 ± 10	17
$\gamma + \varepsilon_{\text{stress-induced}}$	540 ± 20	11.87
Stainless steel	$28,000 \pm 3000$	0

Table 4

Average values of R_p ($\Omega \text{ cm}^2$)

Non-coated SMA	SMA coated by zinc layer	SMA coated by zinc and Cr	316L Stainless steel
450 ± 50	250 ± 20	1550 ± 100	28000 ± 3000

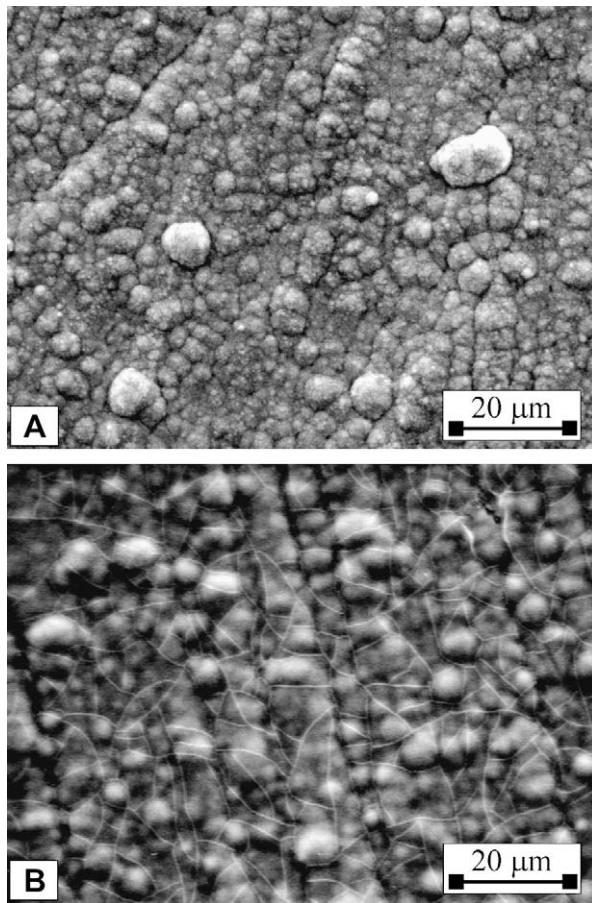


Fig. 3. Microscopic analysis of coatings: (A) SMA electroplated by zinc layer, (B) SMA electroplated by zinc and converted by Cr.

According to the microscopic analyses, we noticed significant differences in the morphologies of deposited coatings. The zinc coating carried out on the studied alloy has a different morphology compared with that usually observed on the ordinary steel substrate [14,15]. Fig. 3A shows a nodular and spongy aspect of coating. As the zinc coating morphology depends on the substrate composition, it is possible that the observed morphology was related to the relatively significant rates of manganese and silicon in the studied alloy.

After conversion coating, the micrographic examination shows a film covering the zinc layer and presenting microcracks (Fig. 3B).

In order to evaluate the anticorrosive performance of the SMA in service, the corrosion of the coated and then prestrained samples, under simulated conditions, was performed in a salt spray chamber. During the test, visual inspections were observed and photographs were taken about every 24 h. Fig. 4 represents photographs

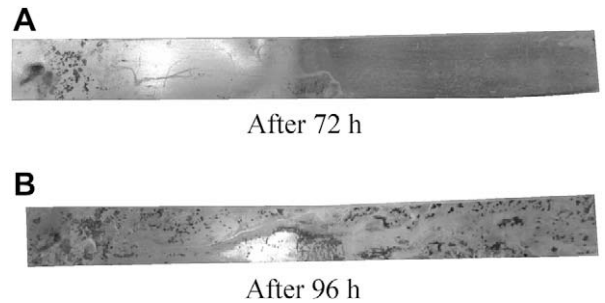


Fig. 4. Results of salt spray tests: (A) after 72 h, (B) after 96 h.

of Zn-electroplated SMA samples finished by chromate conversion treatment and prestrained after 72 h (Fig. 4A) and 96 h (Fig. 4B) of salt spray test. According to these photographs, we can notice that the appearance of white corrosion products at the edges of the sample was visible to the unaided eyes only after 96 h of exposure. This value can be correlated to a suitable actual service performance [10].

3.3. Shape-memory effect

Shape-memory effect tests were carried out before and after coating by using a cylindrical mandrel. The unloading angles, the final angles and the calculated shape memory rates are reported in Table 5. Shape-memory rates given in the same table are average values of three different tests and related to 3.2% prestrain, approximately.

For non-coated alloys, the shape memory rate is equal to 79.2%, which gives a 2.5% recovered strain, approximately. The shape memory rate related to coated SMAs is slightly less significant, but remains acceptable (71.7%, 2.26% recovered strain). These values are usual for iron-based SMAs and can be improved by thermomechanical treatment [16]. The obtained results allow us to draw the conclusion that the protection against corrosion of Fe–32Mn–6Si alloy by zinc-electrodeposited coating, followed by chromate conversion treatment, offers a new possibility of performance improvement of Fe–Mn–Si-based shape-memory alloys for an industrial development.

Table 5
Experimental results of SME

	θ_u (°)	θ_f (°)	r (%)
Non-coated SMA	42	10	79.2
Coated ^a SMA	37	15	71.7

θ_u : unloading angle; θ_f : final angle; r : shape memory ratio.

^a Zn coated followed (or not) by Cr conversion.

4. Conclusion

The results of corrosion investigations of the Fe–32Mn–6Si SMA justify the importance of finding an anticorrosive solution before considering the use of this material in industrial applications.

In this study, we showed, thanks to electrochemical measurements, salt spray tests and SME measurements, that it is possible to protect the Fe–32Mn–6Si SMA against corrosion by zinc-electrodeposited coating achieved by chromate conversion treatment. This suitable anticorrosive treatment, performed before prestrain, protects the alloy after prestrain without impairing its SME performance.

Fe–32Mn–6Si protected by zinc electroplating with chromate conversion treatment can be considered as a potential SMA for industrial applications.

Acknowledgments

A part of this work was realized in the framework of the Cooperation University Joint Committee between France and Tunisia (CMCU Program No. 04S1117). The authors extend their gratitude to their financial support.

References

- [1] T. Bouraoui, K. Tamarat, B. Dubois, *J. Phys.* III 6 (1996) 831.
- [2] A. Sato, E. Chishima, K. Soma, T. Mori, *Acta Metall.* 30 (1982) 1177.
- [3] Z. Dong, W. Liu, D. Wang, J. Chen, D. Liu, *Mater. Sci. Forum* 394–395 (2002) 435.
- [4] H.C. Lin, K.M. Lin, C.S. Lin, T.M. Ouyang, *Corros. Sci.* 44 (2002) 2013.
- [5] O. Soderberg, X.W. Liu, P.G. Yakovenko, K. Ullakko, V.K. Lindroos, *Mater. Sci. Eng.* A273–275 (1999) 543.
- [6] Z. Wang, J. Zhu, *Mater. Sci. Eng.* A358 (2003) 273.
- [7] M. Murakami, H. Otsuka, *Proceedings of the MRS Conference, Tokyo*, vol. 9, 1989, p. 447.
- [8] H. Li, D. Dunne, N. Kennon, *Mater. Sci. Eng.* A273–275 (1999) 517.
- [9] R.G. Kelly, J.R. Scully, D.W. Shoesmith, R.G. Buchheit, *Electrochemical Techniques in Corrosion Science and Engineering*, Marcel Dekker, Inc., New York, 2003, p. 127.
- [10] ASTM B 117-97, *Standard Practice for Operating Salt Spray (Fog) Apparatus*, 1997.
- [11] B.C. Maji, C.M. Das, M. Krishnan, R.K. Ray, *Corros. Sci.* 48 (2006) 937.
- [12] J.H. Yang, H. Chen, C.M. Wayman, *Metall. Trans.* 23A (1992) 1439.
- [13] Z. Xuemei, Z. Yansheng, *J. Mater. Sci. Lett.* 16 (1997) 1516.
- [14] K. Raeissi, A. Saatchi, M.A. Golozar, J.A. Szpunar, *Surface Coatings Technol.* 197 (2005) 229.
- [15] H. Otsuka, *Mater. Res. Soc. Symp. Proc.* 246 (1992) 309.
- [16] K. Tsuzaki, Y. Natsume, Y. Kurokawa, T. Maki, *Scripta Metall. Mater.* 27 (1992) 471.